Inductance Calculation in Interconnect Structures

C. Harlander, R. Sabelka, and S. Selberherr
Institute for Microelectronics, Technical University Vienna
Gusshausstr. 27–29, A-1040 Vienna, Austria, harlander@iue.tuwien.ac.at

Abstract

We present a package based on finite elements for two- and three-dimensional analyses of interconnect structures. Two preprocessors allow a layer-based input of the simulation geometry and the specification of the boundary conditions. Additionally, a third preprocessor provide a fully unstructured three-dimensional grid generation. The tetrahedralization engine uses a modified advancing front Delaunay algorithm. The main module calculates beside the resistances, capacitances and inductances of interconnect structures the distribution of the electric potential, the temperature and the current density. It can be applied for optimization of interconnect structures as well as for studies to verify the reliability of interconnects, as a transient-electric simulation mode [1] is also available to calculate the capacitive crosstalk and delay times. As application example a spiral inductor is analyzed.

Keywords: inductance calculation, multiple integrals, finite element method

1 Introduction

With increasing packaging density and raising signal frequencies inductance effects in interconnect structures gain importance for the electrical behavior of circuits. The largest TCAD commercial vendors present a wide range of solutions for interconnect simulations. These tools (e.g. [2], [3]) have user-friendly and task-oriented interfaces, but still lack some of the features we have incorporated. Our package SAP (Smart Analysis Programs) offers the calculation of, e.g., partial self- and mutual-inductances [4] of interconnect structures. The inductance calculation is based on the computation of the magnetostatic field energy, whereby first the current distributions of the interconnect structures is calculated by means of the finite element method.

2 Physical approach

The influence of the skin effect is neglected, thus results are valid as long as the skin depth $\delta = 1/\sqrt{\mu\gamma\omega}$ is large compared to the diameters of the interconnect structures. μ denotes the magnetic permeability, γ the electrical conductivity and ω the angular frequency. As example: $\delta = 2.6\,\mu m$ for copper at 1 GHz.

The physical details on which our method is based and their numerically consequences are sketched in the following. Because of the universal validity of $\nabla \cdot \mathbf{B} = 0$, we introduce the magnetic vector potential according to $\mathbf{B} = \nabla \times \mathbf{A}$. By choosing the Coulomb gauge $\nabla \cdot \mathbf{A} = 0$, we get

$$-\nabla^2 \mathbf{A} = \mu \mathbf{J} \, . \tag{1}$$

A particular solution of (1) is

$$\mathbf{A}(\mathbf{r}) = \frac{\mu}{4\pi} \int_{V'} \frac{\mathbf{J}(\mathbf{r}')}{|\mathbf{r} - \mathbf{r}'|} dV' \, , \tag{2}$$

where V' is the volume of all conductors. Instead of evaluating the magnetic vector potential in (2) and calculating the energy of the magnetostatic field with

$$W = \frac{1}{2} \int_V \mathbf{J}(\mathbf{r}) \cdot \mathbf{A}(\mathbf{r}) \, dV, \tag{3}$$

we compute the energy directly with the Neumann formula [5]:

$$W = \frac{\mu}{8\pi} \int_V \int_{V'} \frac{\mathbf{J}(\mathbf{r}) \cdot \mathbf{J}(\mathbf{r}')}{|\mathbf{r} - \mathbf{r}'|} dV' dV \, . \tag{4}$$

Pursuing the energy concept leads to the 6-fold integral

$$L_{ik} = \frac{\mu}{4\pi} \frac{1}{I_i I_k} \int_{V_i} \int_{V_k'} \frac{\mathbf{J}_i(\mathbf{r}) \cdot \mathbf{J}_k(\mathbf{r}')}{|\mathbf{r} - \mathbf{r}'|} dV' dV \, , \tag{5}$$

where $\mathbf{r}, \mathbf{r}'$ denotes locations and V_i respectively V_k' the conductive segments, and I_i, I_k are the total currents through these segments. This equation is handled differently, depending whether self-inductances ($i = k$) or mutual-inductances ($i \neq k$) are calculated. Note, that (5) can be simplified by assuming a uniform current density in the conductors. This relates the inductances only to the geometry. However, this results in closed form expressions only for elementary shapes of geometries. Hence, for complex structures with tetrahedral elements the evaluation of the 6-fold integral has to be done numerically.

3 Implementation

3.1 The Program Package SAP

The program package SAP consists of 7 modules. Fig. 1 shows the main tools of the package SAP and displays the data-flow. The simulation is performed with the module STAP (Smart Thermal Analysis Programs [6]) which uses the finite element method to solve the Laplace equation for domains of conducting materials. We obtain the potential distribution by solving the linear equation system with a preconditioned conjugate gradient solver. By applying Ohm's law to the derivative of the electrostatic potential the distribution of the electric current density is obtained.
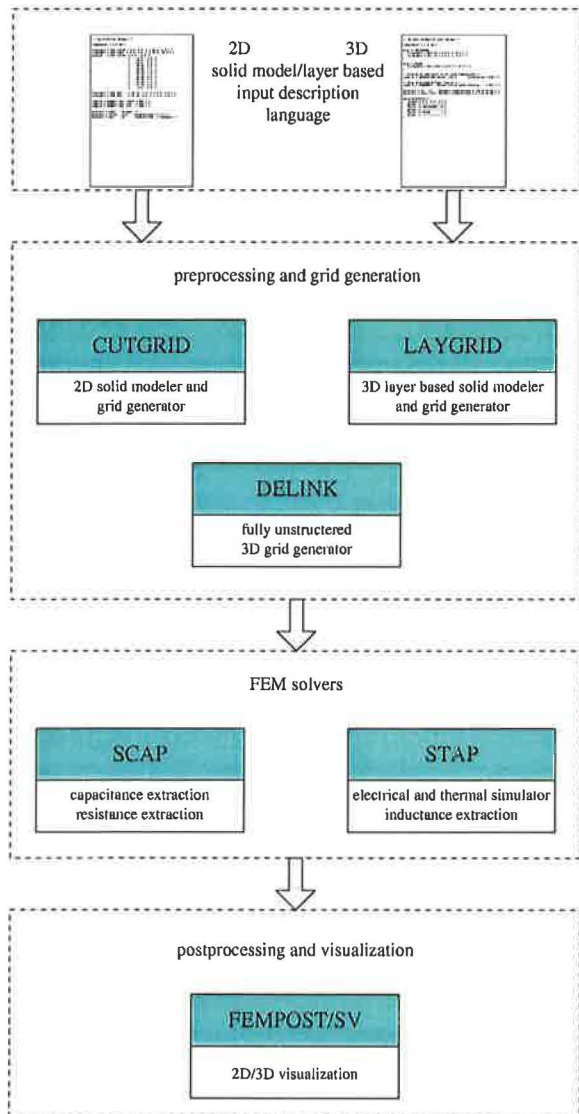

Figure 1: The Smart Analysis Programs

The layout of the interconnect structure can be imported from CIF or GDSII files, or can be created inter-actively with a graphical layout editor [7]. The geometry can be defined either directly from the layout by specifying layer thicknesses, or by a rigorous topography simulation [8], [9]. Furthermore, the program package includes three preprocessors, one for two-dimensional applications (CUTGRID [10]) the other for three-dimensional applications. The meshing strategy of DELINK [11] follows the concept of Delaunay methods. The preprocessed surface description provides the initial front. The preprocessor LAYGRID [12] allows a layer-based input of the simulation geometry with boundary conditions of either Neumann or Dirichlet type specified on the borders of each simulation subdomain. We use tetrahedral grid elements with quadratic shape functions for our layer-based grid generation method. A global grid level refinement is also available as well as a possibility of refinement for an area of interest.

Two postprocessors complete the program package, whereby the visualization tool SV is based on VTK [13]. The second postprocessor FEMPOST can be used to verify the grid quality, and for the visualization of severe distributions (e.g. electric potential, temperature, current density).
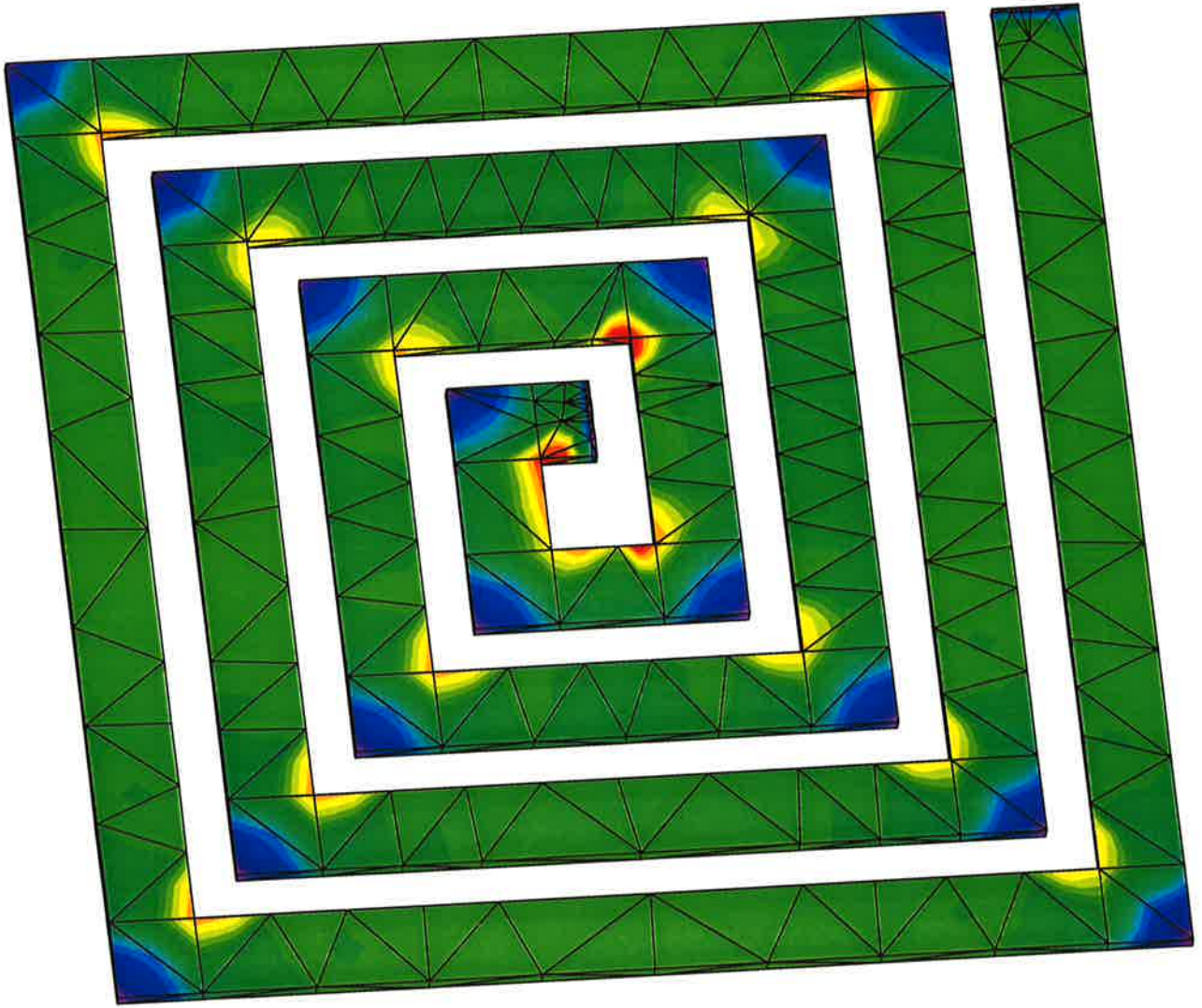
3.2 Mutual Inductances

With the knowledge of the current density we can calculate the magnetostatic field energy to extract the partial inductances. Fig. 2 shows a simple test example and Table 1 the comparison of the results with values received by the formula of Grover [5] as well known reference.
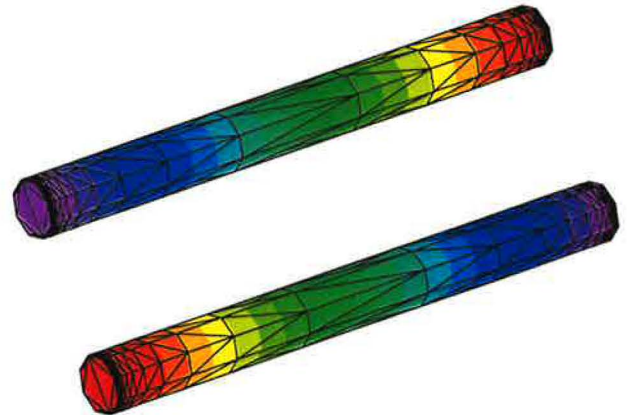
Figure 2: Potential distribution of two parallel conductors with circular cross section

The mutual-inductance is calculated by rewriting the integrations as summations over each element of the conductors i and k. With quadratic shape functions ten nodes per element are used for taking the average of the current density over the element. This is possible, because the term $|\mathbf{r} - \mathbf{r}'|$ is nearly constant if the element

Figure 3: Current density distribution in a spiral inductor

d (cm)	computed (nH)	Grover (nH)
0.1 cm	41.6	41.9
0.3 cm	23.3	23.5
0.5 cm	16.3	16.5
0.7 cm	12.6	12.7

Table 1: Mutual inductance of two conductors (radius is 0.2 cm and the length is 10 cm) with distance d between their centers

size is small compared to the distance between the conductors. Then the term $|\mathbf{r} - \mathbf{r}'|$ can be approximated by the distance between the centers of the elements.

3.3 Self Inductances

For the computation of self inductances more advanced strategies have to be applied. Fig. 3 shows the current density of an spiral inductor, which has following

dimensions: area: 226 x 226 μm, metal width = 18 μm, wire-spacing = 10 μm and the height of the spiral inductor amounts 2.7 μm. The analysis of this example took 27 minutes on an Digital Alpha workstation (DEC600/333 MHz), resulting 2.05 nH for the self inductance. The calculation of the self inductances demand special formulae with certain integration points, published by Stroud [14], who presented various integration formulae which are applicable for various n-simplexes (e.g. the unit triangle, the unit tetrahedron) as integration region. To extract the self-inductances (5) has to be transformed to the unit tetrahedron:

$$L_{ii} = \frac{\mu}{4\pi I_i I_i} \cdot \int_{v \in V_i} \int_{v' \in V_i'} \mathbf{J}_i \left(\mathbf{r} \left(\xi, \eta, \zeta \right) \right) \cdot \mathbf{J}_i \left(\mathbf{r}' \left(\xi', \eta', \zeta' \right) \right)$$

$$\cdot \frac{\det J \det J'}{|\mathbf{r}(\xi, \eta, \zeta) - \mathbf{r}'(\xi', \eta', \zeta')|} \, dv' dv \quad (6)$$

V_i respectively V_i' denote the conductive segments of the ith electrical subsystem, ξ, η, ζ are the local coordinates and $detJ$, $detJ'$ are the transformation determinants, which are not a function of the local coordinates. The kernel of (6) is significant for the behavior of the integral equation, especially if the locations $\mathbf{r}, \mathbf{r}'$ lay in the same tetrahedron it is challenging to compute the integral equation numerically. Thus two strategies are used: For the summations over all different tetrahedrons two formulae with certain integration points are used. According to [15] we utilize the integration formula of the form

$$\int \cdots \int_{S_n} f(x_1, \cdots, x_n) dx_1 \cdots dx_n \stackrel{\circeq}{=} \sum_{i=1}^{N} A_i f(p_i) \quad (7)$$

where S_n is an n-dimensional simplex. The A_i are constants and the $p_i = (p_{i1}, p_{i2}, \cdots, p_{in})$ are points in an n-dimensional space. These points can be obtained from Table I [16] by permutation of the four coordinates

$\nu_1 \quad = 0.0948$
$\nu_2 \quad = \nu_1$
$\nu_3 \quad = 0.2412$
$\nu_4 \quad = 0.5690,$

e.g. $p_{i1} = (\nu_1, \nu_2, \nu_3)$. The second formula applicable to this case is found in [15], formula IV, with the set of points (0,0,0; 1), resp. (1/3,1/3,1/3; 0). This notation denotes the set of points consisting of (0,0,0) and all permutations with 1. These two sets of points are weighted with two different, positive constants. For the interpolation of the current density inside each element the quadratic shape functions are used.

For all summations over identical tetrahedrons an analytic integration in the third coordinate (ζ, ζ') is done, before the two formulae of Stroud [14] for the unit triangle are utilized, namely formula T_n2-1, with the set (0.16,0.16; 0.66) and formula T_n3-6 with the set (0.109,0.232; 0.659), both of them weighted with positive constants.

4 Conclusion

We have presented an advanced method for computing inductances, which was implemented into the package SAP. It allows simultaneous extraction of three-dimensional effective parameters of VLSI circuits.

5 Acknowledgment

REFERENCES

[1] R. Sabelka, R. Martins, and S. Selberherr, "Accurate Layout-Based Interconnect Analysis," in Meyer and Biesemans [17], pp. 336–339.

[2] T. M. A. (now part of Avant!), *RAPHAEL Reference Manual.* 1997.

[3] *TEMPEST Manual.* Santa Clara, California: Silvaco International, 1997.

[4] A. E. Ruehli, "Inductance Calculations in a Complex Integrated Circuit Enviroment," *IBM J.Res.Dev.*, vol. 16, pp. 470–481, Sept. 1972.

[5] F. W. Grover, *Inductance Calculations: Working Formulas and Tables.* D. Van Nostrand Company, New York, 1946.

[6] R. Sabelka and S. Selberherr, "SAP — A Program Package for Three-Dimensional Interconnect Simulation," in *Proc. Intl. Interconnect Technology Conference*, pp. 250–252, June 1998.

[7] R. Martins and S. Selberherr, "Layout Data in TCAD Frameworks," in *Modelling and Simulation*, pp. 1122–1126, Society for Computer Simulation International, 1996.

[8] R. Martins, W. Pyka, R. Sabelka, and S. Selberherr, "High-Precision Interconnect Analysis," *IEEE Trans.Computer-Aided Design*, vol. 17, no. 11, pp. 1148–1159, 1998.

[9] W. Pyka, R. Martins, and S. Selberherr, "Efficient Algorithms for Three-Dimensional Etching and Deposition Simulation," in Meyer and Biesemans [17], pp. 16–19.

[10] R. Bauer and S. Selberherr, "Preconditioned CG-Solvers and Finite Element Grids," in *Proc. CCIM*, vol. 2, Apr. 1994.

[11] P. Fleischmann, W. Pyka, and S. Selberherr, "Mesh Generation for Application in Technology CAD," *IEICE Trans.Electron.*, vol. E82-C, no. 6, pp. 937–947, 1999.

[12] P. Fleischmann, R. Sabelka, A. Stach, R. Strasser, and S. Selberherr, "Grid Generation for Three Dimensional Process and Device Simulation," in *Simulation of Semiconductor Processes and Devices*, pp. 161–166, Business Center for Academic Societies Japan, 1996.

[13] W. Schroeder, K. Martin, and B. Lorensen, *The Visualization Toolkit: An Object-Oriented Approach to 3D Graphics.* Prentice-Hall, 1996.

[14] A. H. Stroud, *Approximate Calculation of Multiple Integrals.* Prentice-Hall, Englewood Cliffs, N.J., 1971.

[15] A. H. Stroud, "Some Approximate Integration Formulas of Degree 3 for an n-Dimensional Simplex," *Numer.Math.*, vol. 9, pp. 38–45, 1966.

[16] A. H. Stroud, "Approximate Integration Formulas of Degree 3 for Simplexes," *Math.Comp.*, vol. 18, pp. 590–597, 1964.

[17] K. D. Meyer and S. Biesemans, eds., *Proc. Simulation of Semiconductor Processes and Devices*, Springer, Sept. 1998.